Review

DNA-based enzymatic systems and their applications

Yunfei Jiao,[1,2,4] Yingxu Shang,[1,4] Na Li,[1,2,*] and Baoquan Ding[1,2,3,*]

SUMMARY

DNA strands with unique secondary structures can catalyze various chemical reactions and mimic natural enzymes with the assistance of cofactors, which have attracted much research attention. At the same time, the emerging DNA nanotechnology provides an efficient platform to organize functional components of the enzymatic systems and regulate their catalytic performances. In this review, we summarize the recent progress of DNA-based enzymatic systems. First, DNAzymes (Dzs) are introduced, and their versatile utilities are summarized. Then, G-quadruplex/hemin (G4/hemin) Dzs with unique oxidase/peroxidase-mimicking activities and representative examples where these Dzs served as biosensors are explicitly elaborated. Next, the DNA-based enzymatic cascade systems fabricated by the structural DNA nanotechnology are depicted. In addition, the applications of catalytic DNA nanostructures in biosensing and biomedicine are included. At last, the challenges and the perspectives of the DNA-based enzymatic systems for practical applications are also discussed.

INTRODUCTION

DNA nanotechnology has been flourishing since the pathbreaking fabrication of the first immobilized 4-arm DNA junction reported by Seeman and co-workers in 1982 (Seeman, 1982). Based on the seminal DNA tiles, various complex DNA nanostructures have been successfully assembled, including the DNA tile (Fu and Seeman, 1993), the double crossover (DX) structure (Liu et al., 2011), the single-stranded tile (SST) (Wei et al., 2012), the DNA origami (Rothemund, 2006; Tikhomirov et al., 2017), and so on . DNA origami has attracted significant attention in fabricating more complex structures with controlled sizes and shapes. The DNA origami nanostructure is assembled by the annealing process where a long single-stranded DNA (ssDNA) scaffolds (usually M13mp18 genome DNA) is folded into predesigned geometries by ∼200 complementary short ssDNA (Rothemund, 2006). Up to now, the development of DNA nanotechnology with high programmability and addressability has promoted the fabrication of one-dimensional (1D), two-dimensional (2D), and three-dimensional (3D) DNA nanostructures (Vázquez-González et al., 2020). The extraordinary properties possessed by DNA nanostructures, including great biocompatibility and programmability, enable their wide applications in materials science and biomedical studies. A particularly fascinating part of DNA nanotechnology is the DNAzymes (Dzs), which refer to a class of DNA nanostructures with excellent catalytic abilities to catalyze multiple reactions. The first DNA-based catalyst was reported by Ronald Breaker and Gerald Joyce in 1994 (Breaker and Joyce, 1994). In their pioneer work, DNA strands with unique secondary structures can catalyze the transesterification of RNA phosphate diester bonds. Since then, a plethora of artificial DNA sequences as active enzymes were selected by Systematic Evolution of Ligands by Exponential enrichment (SELEX), which has become an important technology for Dzs library screening due to its excellent target analysis range and strong affinity (Silverman, 2016; Kumar et al., 2019; Wang et al., 2021a). Regioselective Dzs consisting of synthetic DNA single stands and different cofactors have been developed with diverse catalytic abilities (Kumar et al., 2019; Hollenstein, 2015), e.g., DNA/RNA cleavage or ligation (Zhou et al., 2015, 2016; Praetorius et al., 2017; Wu et al., 2017; Huang et al., 2020; Purtha et al., 2005), phosphorylation (Camden et al., 2016), hydrolysis (Chandra et al., 2009), and alkyne-azide "click" cycloaddition (Liu et al., 2020a). Considering the versatility in terms of catalytic mechanisms, Dzs have shown promising potentials for biosensing, theranostics, and biomedicine, etc. (Huang et al., 2020; Liu et al., 2017a; Yousefi et al., 2018; Zhang et al., 2020; Peng et al., 2017; Wei et al., 2020). Meanwhile, Dzs have advantages over protease and ribozyme due to the easy fabrication, low cost, storage convenience, and high stability (Hollenstein, 2015; Guo et al., 2017). In 1998, Travascio et al. reported a hemin-G4 Dz consisting of hemin and G4 with enhanced horseradish

peroxidase (HRP)-like activity (Travascio et al., 1998). In this catalytic system, hemin not only possesses inherent HRP-like activity but also works as an active cofactor of this designed artificial enzyme. In the presence of metal ions, guanine (G)-rich single-stranded short DNA sequences can bind to hemin tightly via the formation of intramolecular G4, forming hemin-G4 Dzs. Peroxidase-mimicking G4 Dzs have drawn wide attention as a substitution to natural HRP, thereby avoiding the intrinsic problems faced by the natural proteins, e.g., instability and difficulty in modification (Morrison et al., 2018). Therefore, the hemin-G4 Dzs have been successfully applied in the detection of biomarkers, microorganisms, biotoxins, and metal ions (Wang et al., 2014; Hoang et al., 2015; Li et al., 2016; Liu et al., 2017b; Winterwerber et al., 2020).

Besides, DNA molecules can contribute to the assembly of DNA nanostructures with reasonable and precise design (Vázquez-González et al., 2020). Plenty of DNA nanostructures or DNA-based nanoplatforms have been fabricated with various sizes, morphologies, and dimensions by the accurate arrangement of diversified DNA sequences. The DNA-based nanostructures provide platforms to immobilize catalytic enzymes and conduct cascade reactions. DNA nanoplatforms with 1D, 2D, and 3D structures have been designed and fabricated to meet the need for DNA-based enzymatic cascade systems, for instance, wrapping enzymes for protection, and providing a fixed platform to examine the catalytic mechanism, etc. (Fu et al., 2014; Linko et al., 2015; Ngo et al., 2016; Chen et al., 2018b; Yang et al., 2019).

In this review, we aim to summarize the recent progress of Dzs into five parts: (1) the Dzs classified by their different catalytic functions are firstly introduced, e.g., nucleotide cleavage and ligation, DNA phosphorylation, and so on (Praetorius et al., 2017; Cuenoud and Szostak, 1995; Ponce-Salvatierra et al., 2016; Santoro and Joyce, 1997); (2) the hemin-G4 Dzs, as a commonly used enzyme mimicking nanostructures, are summarized in the second part; (3) the DNA-based enzymatic cascade systems, involving 1D, 2D, and 3D cascade reaction platforms based on DNA nanostructures, are discussed in the third part; (4) the prospective applications of Dzs in biosensing and biomedicine are summarized in the following part; (5) the challenges and future development trends in applying DNA molecules in building novel catalytic platforms are finally discussed.

THE FUNCTIONS OF DZS

Since the first Dz reported by Ronald Breaker and Gerald Joyce in 1994 (Breaker and Joyce, 1994), many kinds of Dzs for catalysis have been explored and synthesized. The sequences of Dzs and the cofactors determine the functions of Dzs, which can be employed to catalyze various chemical reactions, such as ligation and cleavage of nucleotides and DNA phosphorylation, etc. In this part, we will summarize various Dzs according to their different catalytic functions.

DNA/RNA ligation

In 1995, Cuenoud et al. firstly screened and discovered a 47 nt long Dz, which is able to catalyze the formation of new phosphodiester bonds, and initiates the ligation between different DNA sequences (Cuenoud and Szostak, 1995). Since then, more and more Dzs have been developed for the ligation of DNA or RNA. Normally, Dzs with DNA ligase activity catalyze the ligation between two DNA sequences. This reaction requires the imidazole group to be attached to the phosphate group at the 3′ end of one DNA fragment for guaranteeing the ligation with the 5′ end of the other DNA strand. Similarly, the ligations between RNA strands by Dzs have also been reported. In 2005, Purtha and coworkers identified two kinds of Dzs via *in vitro* selection, which are specific to Mg^{2+} and Zn^{2+}, respectively (Purtha et al., 2005). Both of them with 40 nt long DNA strand catalyze the linkage between two RNA substrates and allow various changes at the sites far away from the ligation sites on RNA substrates, as depicted in Figure 1A. These two kinds of Dzs possess higher capabilities on catalyzing 3′-5′ RNA linkages with relatively substantial yield and are suitable to prepare long RNAs. In order to realize the optimal design of Dzs to develop their potential applications in biomedicine, many efforts on the study of the basic mechanism of their functions have been conducted. Pena et al. analyzed the 3D crystal structure of a Dz specified to Mg^{2+} (named 9DB1) in 2016 for the first time (Ponce-Salvatierra et al., 2016). The revealed crystal structure preliminarily verifies that specific DNA strands have the ability to realize tertiary folds to function catalytic activity. Afterward, Orozco's group revealed the mechanism of RNA linkage catalyzed by 9DB1 experimentally and theoretically, which offers more insights into the knowledge of key nucleotides in full sequences of Dzs and cofactors, improving the design of novel and effective Dzs with ligase-like activity (Aranda et al., 2019). Furthermore, the Dzs-catalyzed oligonucleotide 3′-phosphorylation has been elaborately studied. Li and coworkers have already isolated nearly 50 kinds of DNA strands with polynucleotide kinase-like activity in 1999 (Li and Breaker, 1999).
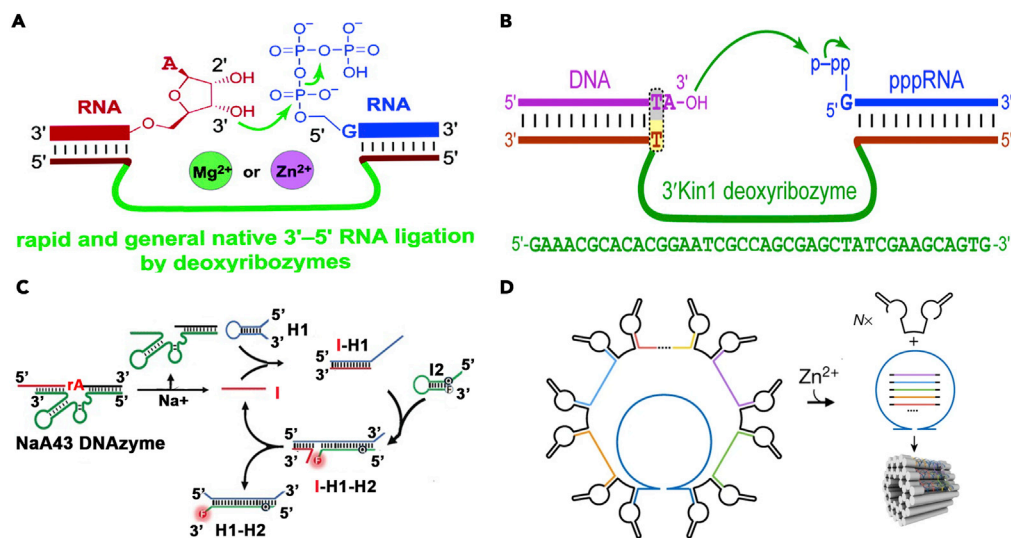
Figure 1. The Dzs with different catalytic performances
(A) Schematic illustration of DNA-catalyzed 3′–5′ RNA ligation. Reproduced with permission (Purtha et al., 2005). Copyright 2005, American Chemical Society.
(B) Scheme of DNA-catalyzed oligonucleotide 3′-phosphorylation. Reproduced with permission (Camden et al., 2016). Copyright 2016, American Chemical Society.
(C) Scheme of a Dzs-catalytic NaA43 hairpin assembly (DzCHA) probe. Reproduced with permission (Wu et al., 2017). Copyright 2017, Elsevier.
(D) Scheme of DNA-cleaving Dzs-guided self-excising cassettes to produce staple strands and scaffold for DNA nanostructure assembly. Reproduced with permission (Praetorius et al., 2017). Copyright 2017, Nature Publishing Group.

Then, for a further and detailed exploration, Alison et al. identified a kind of Dz that enables DNA oligonucleotide 3′-phosphorylation, wherein 5′-triphosphorylated RNA transcript (pppRNA) provides phosphoryl, as is demonstrated in Figure 1B (Camden et al., 2016). The obtained Dzs, named 3′ Kin1, realizes the 3′-phosphorylation of theoretically all DNA substrates with motif 5′-NKR-3′ at 3′ end (N is oligonucleotide sequence, K is T or G, and R is A or G). Surprisingly, the mutation from A to T of the first sequence of 3′Kin1 induces unpredictable optimal activity. Here, they succeeded in verifying the feasibility of selecting Dzs for oligonucleotide 3′-phosphorylation via *in vitro* selection.

Nucleotide-cleavage Dzs

RNA-cleavage Dzs

In the following part, we summarize two most commonly used Dzs with cleavage functionalities, i.e., RNA cleavage and DNA cleavage. Since the first RNA-cleavage Dzs (RCD) revealed by Breaker and Joyce in 1994 (Breaker and Joyce, 1994), various Dzs have been extracted or synthesized for cleaving specific sites of RNA, resulting in inactive genes at mRNA level to regulate the expression of related proteins (Wang et al., 2021a, 2021b; Meng et al., 2019). Due to their precise mRNA regulation functions, RNA-cleavage Dzs play a significant role in treating RNA viruses and other diseases such as tumors. The representative RCDs, including 8–17 type and 10–23 type, were firstly reported by Joyce's group (Santoro and Joyce, 1997). Typical 8–17 Dzs with a catalytic core of 14 nucleotides can cleavage RNA at the sites extended from A-G into N-G (N indicates A/U/C/G) with divalent metal ions as cofactors (Brown et al., 2003). Except for catalyzing pyrimidine to form pyrimidine junctions, 8–17 Dzs show excellent catalytic activity to other functional groups comprising purine and pyrimidine (Schlosser et al., 2008). Based on the valid RNA cleavage ability of 8–17 Dzs, Yu et al. induced phenyl boronate (BO) and phosphorothioate (PS) to modify Zn^{2+}-dependent 8–17 Dzs, which can be activated by intracellular reactive oxygen species (ROS) (Xiao et al., 2019). BO embedded at the catalytic core can be removed by endogenous hydrogen peroxide (H_2O_2) to recover the activity of BO-Dzs. Likewise, endogenous hypochlorous acid (HClO) cleaves PS incorporated at the site linked with a blocking sequence. Via these ways, BO-Dzs and PS-Dzs can be activated by H_2O_2 and HClO coexisting in both murine cells and human cells.

Taking advantage of 10–23 Dzs' high specificity for Mg^{2+} and high efficacy for RNA cleavage, Lin et al. reported a 10–23 Dzs-based biosensor with an 18-base pair recognition site that can recognize homing endonuclease (Lin et al., 2019). The endonuclease can cleave this 18-base pair recognition region to recover the active configuration of Dzs to recognize their cofactor Mg^{2+}. Meanwhile, the Mg^{2+} triggers the Dzs-mediated cleavage to release the DNA sequences tagged with a fluorophore, resulting in the change of fluorescent signals. Therefore, this 10–23 Dzs-based biosensor can be used for intracellular imaging of Mg^{2+}. In 2019, Li's group delivered a nanohybrid consisting of 10–23 Dzs and Cu^{2+} for synergistic tumor therapy (Liu et al., 2021a). The 10–23 Dzs released from the nanohybrids can catalyze the vascular endothelial growth factor-2 (VEGFR2) mRNA cleavage and then trigger the gene silencing, together with Cu^+-mediated hydroxyl radicals ($\cdot$OH) generation for chemodynamic therapy. Generally, the 10–23 Dzs can be designed to target almost any substrates at the RNA purine-pyrimidine junction, allowing the modulation of gene expression and tumor treatment by regulating the expression of intracellular RNAs (Khachigian, 2019). Among RCDs, one type of Dzs have been designed based on monovalent metal ions rather than divalent metal ions as the cofactors, enriching the functions of Dzs with the detection of monovalent metal ions (Torabi et al., 2015). Zhou et al. reported Na^+-dependent RCDs obtained by a choreographed *in vitro* selection (Zhou et al., 2016). The designed DNA strands include a single adenine ribonucleotide (rA), which facilitates the susceptible RNA cleavage. It is noteworthy that this type of Dzs keeps active in different kinds of chemical environments, including 54% alcoholic solvents, and only required Na^+ as the cleavage cofactor. In addition, the designed Dz is still active at a relatively low concentration of Na^+ and a high concentration of ethanol (72%) or dimethylsulfoxide (DMSO). The catalytic rate in such organic solvent is 1000-fold higher than that in water. This kind of Dzs can be applied in the detection of the alcohol content, which has a comparable detection performance to the commercial methods.

Lu's group fabricated a biosensor based on the NaA43 Dzs combining catalytic hairpin assembly (CHA) to measure Na^+ content (Figure 1C) (Wu et al., 2017). This biosensor named DzCHA can cleave the substrates at rA and release hairpin DNA (H1) and short sequence DNA strands (I, red line) in the presence of Na^+, thereby recovering the fluorescence. The fluorescence intensity is proportional to the Na^+ concentration. For intracellular detection, the rA portion is modified with a UV-light-sensitive group, 2'-O-nitrobenzyl adenosine (PG), forming the photocaged substrate strand of the NaA43 Dzs. The ultraviolet light removes the PG and then relieves the rA portion from the photocaged substrate strand of the NaA43 Dzs, thus realizing a controllable activation of DzCHA probe. It is found that the combination of the feasible DzCHA probe and additional Na^+ can trigger the strongest fluorescence signals, indicating that this DzCHA probe can serve as the universal strategy for DNA-based sensors to enhance the detective signals, which is helpful to further study the functions of metal ions in complicated biological environments.

DNA-cleavage Dzs

Another nuclease selected for DNA cleavage is referred to as DNA-cleavage Dzs (DCD), which was reported as early as 2009 by Chandra (Chandra et al., 2009). They isolated a DNA-hydrolysis DCD with an accelerated rate of 10^8, and subsequently, they inserted an Ala-Ser-Ala tripeptide sequence to the 40 nt long DNA region to cleave amide bonds. This pioneering work for the selection of DNA-hydrolysis Dzs represents a milestone in the field of catalytic nucleic acids.

Besides the applications in sensing, imaging, or cancer therapy, DCDs can also make contributions to the synthesis of various nanostructures. For instance, Dietz's group reported a DCD-assisted strategy for mass production of DNA nanostructures (Praetorius et al., 2017), as shown in Figure 1D. The required DNA staples (colored line) and the Zn^{2+}-dependent self-cleaving Dzs (black line) are cloned into phagemid backbones for amplification. In the presence of Zn^{2+}, the produced amplicons can be cleaved and release multiple staples and scaffold, thereby realizing a mass production of target structures. The feasibility of producing desirable sequences obtained by cleavage DNA strands with DCDs will allow the mass production of DNA nanostructures at low costs, which lay the foundation for future commercial use.

G4 WITH PEROXIDASE-MIMICKING ACTIVITY

The integration of G4 and hemin or porphyrin analogue exhibits HRP-like activity, and the assembled structure can be regarded as hemin-G4 Dzs. Compared with the natural peroxidase, HRP-mimicking Dzs take the advantages of higher stability and compatibility, easier modification and synthesis. Therefore, they are utilized in many fields, such as biosensors, nanostructure fabrication and DNA nanomachines (Mergny and Sen, 2019). For instance, Kurapati et al. used an 18 nt long DNA sequence combined with porphyrin
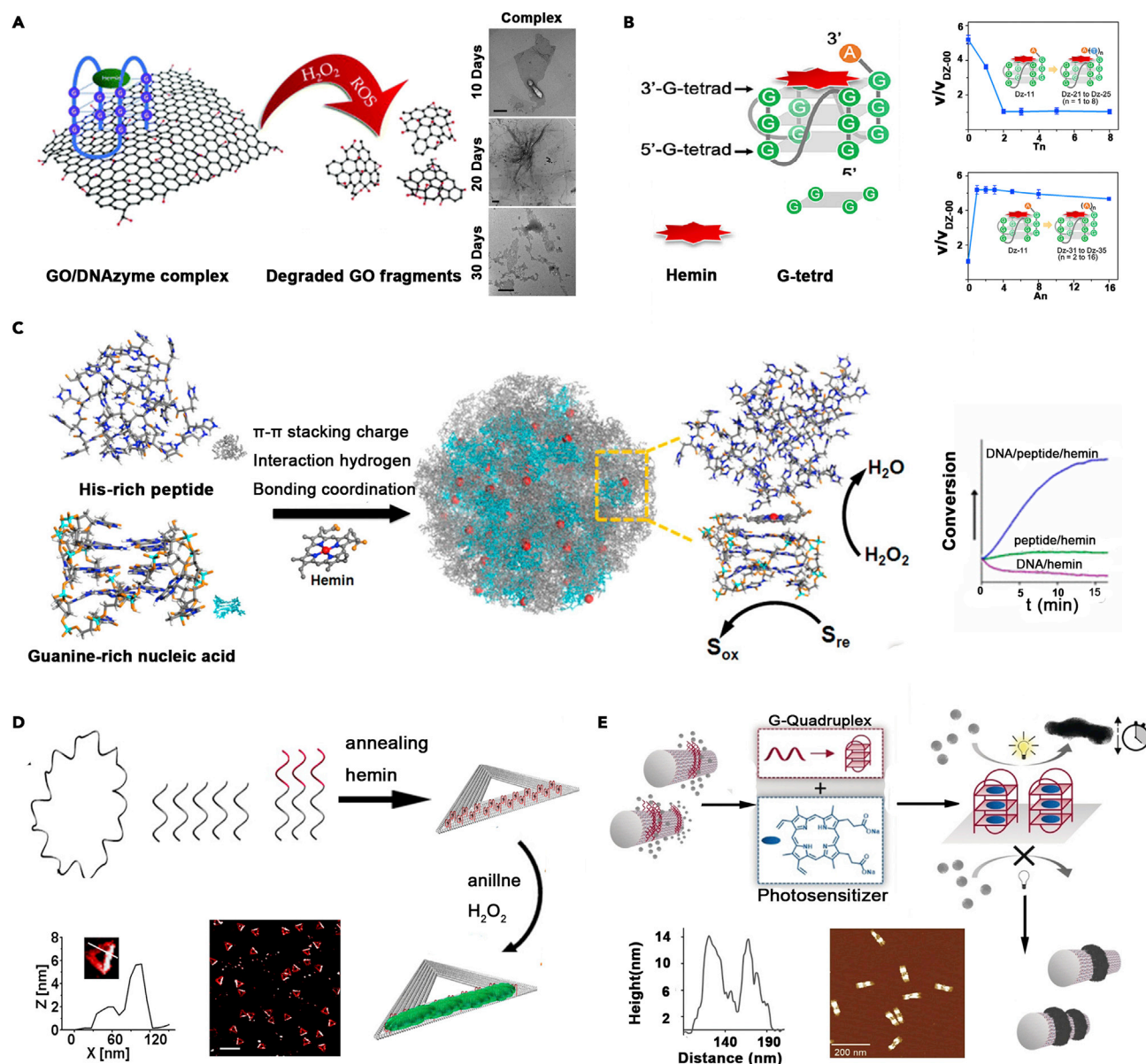
Figure 2. G4/hemin Dzs with enhanced HRP-like activity

(A) Degradation of GO induced by PS2.M–hemin complex. Scale bar: 500 nm. Reproduced with permission (Kurapati and Bianco, 2018). Copyright 2018, Royal Society of Chemistry.

(B) The Dz-11-hemin complex used for enhanced enzymatic systems. The influences of different factors on enhancement effect of the adjacent adenine (EnEAA effect): (Upper right) the different length of poly-T spacer and (Lower right) poly-A at 3' terminal of G4 sequence. Reproduced with permission (Li et al., 2016). Copyright 2016, Oxford Academic.

(C) Self-assembly and the catalytic performance of peroxidase-mimicked nanoparticles consisting of G-rich nucleic acid, His-rich peptide, and hemin. Reproduced with permission (Liu et al., 2017b). Copyright 2017, American Chemical Society.

(D) Site-selective synthesis of polyaniline (PANI) on triangular DNA origami based on G4 Dzs. Scale bar: 200 nm. Reproduced with permission (Wang et al., 2014). Copyright 2014, American Chemical Society.

(E) Light-triggered polydopamine formation on DNA origami by G4 Dzs catalysis. Reproduced with permission (Winterwerber et al., 2020). Copyright 2020, Wiley-VCH.

moiety of hemin to oxidize and degrade graphene oxide (GO) in the presence of H_2O_2, as shown in Figure 2A (Kurapati and Bianco, 2018). The hemin-based Dzs catalyze H_2O_2 oxidation in the form of two-electron mechanism (Poon et al., 2011), resulting in the generation of reactive oxygen intermediates (ROS); for the two-electron oxidation mechanism of the hemin-based Dzs: two successive one-electron oxidations,

named "oxygen rebound mechanism," that proceed via a substrate radical intermediate (oxoiron [IV] porphyrin cation radicals). It is operated in most hemin-based Dzs (Poon et al., 2011). In the mentioned work, the produced ROS initiates the oxidation reaction on the defects or edges of GO, causing progressive holes on GO surface, as is shown in the TEM images in Figure 2A (Kurapati and Bianco, 2018). This novel hemin/G4 Dzs with better stability is capable of efficiently eliminating GO or other carbon nanomaterials, which is of great value for the further application of carbon-based nanomaterials in the field of biomedicine and relative industry. Recently, Belcher's group proposed an efficient approach to cut the single-wall carbon nanotubes (SWNTs) with controlled length by using the DNA origami and G4-hemin Dzs hybrids (Atsumi and Belcher, 2018). The hybrids are synthesized by immobilizing the hemin/G4 Dzs-wrapped SWNTs onto the predesigned sites of the DNA origami via the biotin-streptavidin recognition. In the presence of H_2O_2, the HRP-like hemin/G4 Dzs facilitate the decomposition of H_2O_2 to generate free radicals that triggers the cleavage of SWNT at G4-hemin Dzs existing sites. Accordingly, the pinpointed hemin/G4 Dzs on the DNA origami realizes the rapid and efficient cutting of SWNTs with required lengths, which can be further applied in the studies of quantum mechanics and the synthesis of nanopore-based sensors.

Recently, various methods have been explored to meet the need of improving catalytic activity of hemin-based Dzs for further applications. Yao's group tried to add 3 adenines (A) into the Dzs to improve the activity of G4 Dzs via the intramolecular enhancement effect of the adjacent adenine (EnEAA) effect (Figure 2B) (Li et al., 2016). By adding A bases at 3'-end of DNA core sequence, the purine N1 atom and exocyclic 6-amino groups of adenine accelerate the formation of the intermediate and critical active substance during the catalytic process, causing a 5- to 20-fold enhancement of activity compared with original hemin-based G4 Dzs. Different amounts of thymine (T) inserted at the 3'-end of the G4 core sequence result in a declined activity with the increasing number of T bases. It indicates that only the adjacent A facilitates the EnEAA effect, as is shown in Figure 2B (lower right). Similarly, in 2017, Zhou's group reported that G4 Dzs possess intensive activity and perform length-dependent effects when the loop domains are A or C bases (Chen et al., 2017). They found that the repeated dA nucleotides, which work as the linkers and loop sequences in the loops of parallel G-quadruplex, accelerate the intermediate formation to speed up the catalytic process. The insertion of different nucleobases, especially dA, at the terminal of G4 was subsequently demonstrated to greatly improve the catalytic activity of G4/hemin Dzs. This strategy also provides an idea for designing the thermophilic and high-active G4/hemin Dzs by using the addition of dA at the terminal of the G4 (Guo et al., 2017). Afterward, inspired by the π-π stacking conjugation between hemin and G4, Zhou's group managed to modulate the activity of G4/hemin Dzs by modifying the flanking sequence close to the terminal plane of G4 (Chen et al., 2018a). The highly active G4/hemin Dzs are expected to be used in biosensors to realize desirable sensitivity. Subsequently, the improved catalytic performance of G4-Dzs was achieved via the chemical modifications of the DNA backbone that provide G4 with double 3'-external G-quartets (Virgilio et al., 2020). Virgilio et al. introduced a G4 Dz consisting of two G4 with similar 3'-terminals (Virgilio et al., 2020). The increased 3' end promotes the affinity of hemin, resulting in an intensive catalytic ability. Recently, Wang et al. also proposed that the embedded external quartet was in favor of the enhanced affinity to hemin and activation of the iron atom in hemin (Wang et al., 2020). Moreover, the addition of histidine-rich peptides can also contribute to enhanced enzymatic activity (Liu et al., 2017b, 2020b; Du et al., 2021, 2022), as is shown in Figure 2C. Van der Waals force drives histidine-rich peptides to assemble with G-rich Dzs for capturing hemin. The stacking state of hemin presented at the terminals of folded G-rich Dzs allows more hemins to be exposed to H_2O_2, resulting in the enhanced catalytic activity. Furthermore, amino acid residues of histidine embed hemin to protect it from oxidative degradation. The synergistic effect of histidine and hemin accounts for the reasonably improved catalytic performance.

Taking advantage of the HRP-like activity, hemin/G4 Dzs with negative charges hold the potential to assist the synthesis of polyaniline (PANI). PANI is of great significance in electronics and energy storage. Negatively charged polyelectrolyte is commonly used as the template for PANI growth. Wang and coworkers developed a method for PANI growth on 2D triangular DNA origami (TOA) with controlled shape by the guidance of HRP-mimicking hemin/G4 Dzs (Figure 2D) (Wang et al., 2014). The addressability of DNA origami furnishes hemin/G4 Dzs with designed sites on TOA. In the presence of aniline and H_2O_2, Dzs at the specific position on the TOA catalyze the oxidation of aniline into aniline radicals, followed by the subsequent growth of PANI. The AFM images and the height of the synthesized PANI structures verified the successful growth of PANI on 2D TOA (Figure 2D). Subsequently, Weil's group proposed a Dz catalyzed method for the polymerization of dopamine (Winterwerber et al., 2020). They synthesized a tubular DNA
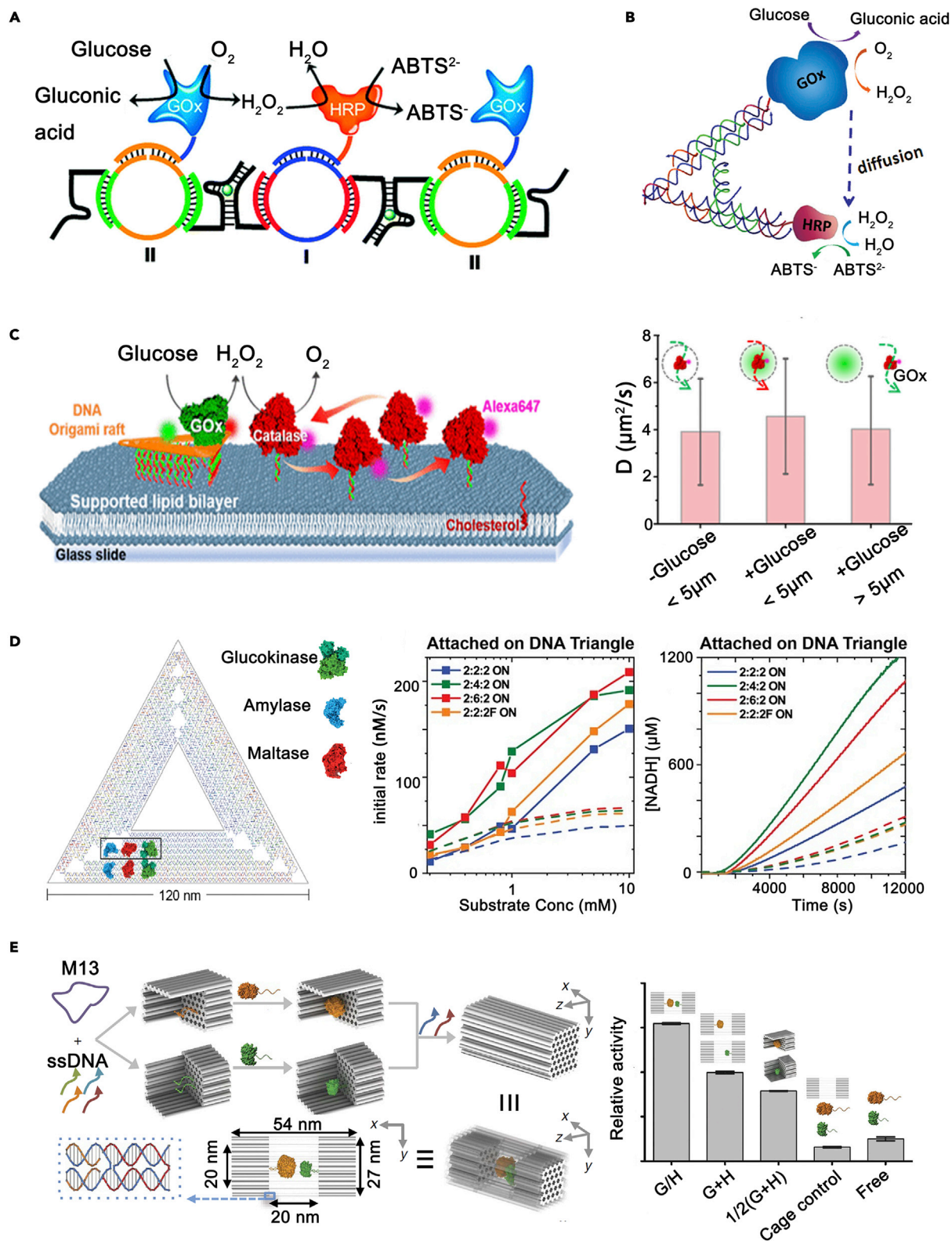
Figure 3. DNA-nanostructure-based enzymatic cascade reaction systems

(A) Illustration of HRP/GOx bi-enzymes biocatalytic cascade on the DNA nanowire. Reproduced with permission (Wang et al., 2009). Copyright 2009, American Chemical Society.

Figure 3. *Continued*

(B) Scheme of reversible regulation of enzyme cascade reaction by a DNA nanomachine. Reproduced with permission (Xin et al., 2013). Copyright 2013, Wiley-VCH.

(C) HRP/GOx enzymatic cascade on 2D DNA origami raft for real-time imaging at the single-molecule level under the different distances of immobilized GOx. The green and red arrow refer to Brownian motion and enhanced motion, respectively. Reproduced with permission (Sun et al., 2017). Copyright 2017, American Chemical Society.

(D) Co-assembled amylase, maltase, and glucokinase on triangular DNA origami for enzymatic cascade reaction with enhanced catalytical activity. Reproduced with permission (Klein et al., 2019). Copyright 2019, American Chemical Society.

(E) Schematic illustration of DNA nanocage-encapsulated bi-enzymes system (GOx, orange; HRP, green) and the activity analysis of encapsulated GOx/HRP pairs. Reproduced with permission (Zhao et al., 2016). Copyright 2016, Nature Publishing Group.

origami and settled the G4 Dzs at the specific sites to form the lined or the dotted patterns. The G4 Dzs extensions act as the anchor sites for capturing the photosensitizer protoporphyrin IX (PPIX), a kind of hemin analogue (Figure 2E). With irradiation of the visible light, PPIX induces the generation of ROS and conducts the following dopamine oxidation at the specific sites. The light-mediated polymerization of dopamine on 3D DNA origami succeeds in synthesizing well-defined nanostructures with spatiotemporal control. Furthermore, the uniform deposition of polydopamine can enhance the stability of tubular DNA origami in the solution without cations. Therefore, through manipulating hemin (or its analogies)/G4 Dzs to optimize their functions and activities, this kind of DNA-based enzymatic system may generate broad applications in biosensing, cancer therapies, and chemical reactions (Zhong et al., 2018; Sun et al., 2019; Xu et al., 2021).

DNA-BASED ENZYMATIC CASCADE SYSTEMS

Taking advantage of the outstanding programmability and high biocompatibility, DNA nanostructures have become promising candidates as the platform to load functional enzymes to fabricate stable, position- and shape-controlled DNA-based enzymatic cascade systems. Plenty of 1D, 2D, and 3D DNA nanostructures as enzyme immobilizing platforms for cascade reactions have been reported. The well-designed DNA-based enzymatic cascade systems avail the further application and property study. A present landscape relevant to the fabrication and application of the enzymatic cascade systems based on DNA nanostructures as the templates is described in this section.

Enzymatic cascade systems based on 1D DNA nanostructures and DNA tiles

The original DNA-based cascade enzymatic systems are fabricated on the scaffold of DNA tiles or 1D DNA nanostructures. Wang et al. reported a 1D DNA nanowire obtained by the self-assembly of two kinds of circular DNA moieties to organize glucose oxidase (GOx) and HRP, as is shown in Figure 3A (Wang et al., 2009). Due to the high local concentration caused by the well-designed positioning of bi-enzymes, the cascade reaction is activated by the addition of glucose. The catalytic rate of these enzymatic cascade systems based on 1D DNA nanostructures is 6-fold higher than that caused by free bi-enzymes without the DNA platform. Simple DNA nanostructures with precise design (e.g., DNA tiles) show potential in serving as the platform to load enzymes and performing the cascade reaction. A DNA nanomachine reported by Liu's group in 2013, which loaded bi-enzyme (GOx and HRP) on two arms of a single DNA tile, can realize the reversible control of the cascade reaction (Figure 3B) (Xin et al., 2013). The strategy of strand displacement reaction is used to incorporate a DNA motor into the middle of the DNA machine. The DNA motor assists the DNA machine in switching back and forth between open and close states, resulting in the distance change between bi-enzymes, thereby regulating the cascade reaction. This strategy provides the possibility for the subsequent study of DNA machines with more complex functions and different response mechanisms to realize the modulation of multi-enzyme biosystems and facilitates follow-up explorations of other distance-dependent biosystems.

Enzymatic cascade systems based on 2D DNA nanostructures

2D DNA nanostructures can also be used to investigate distance-dependent cascade reactions in confined spaces. For instance, Fu et al. evaluated the effect of the distance-dependent kinetic process of bi-enzymes systems between GOx and HRP located on a confined rectangular DNA origami, as the distance changed from 10 nm to 65 nm (Fu et al., 2012). They observed that the shorter distance between bi-enzymes resulted in stronger catalytic activity due to a relatively close distance. It allows the intermediates to transfer from GOx to HRP along the protein surface instead of diffusing in the bulk solution. Thus, the high local concentration of intermediates leads to a significantly enhanced catalytic performance. Later, Fan's group developed a raft-based platform

using the triangular DNA origami for real-time imaging of enzymatic cascade at the single molecular level (Sun et al., 2017). As demonstrated in Figure 3C, the upstream enzyme (GOx) is immobilized onto the cholesterol-labeled triangular DNA origami raft, and the downstream enzyme (HRP) is anchored on the cholesterol-labeled dsDNA intercalated in the supporting lipid bilayer. The average diffusion velocity of catalase under the different distances of immobilized GOx was illustrated in the right image in Figure 3C. Within a given diameter range of 5 μm of GOx, HRP performs a simple Brownian motion in the absence of substrate glucose. However, the addition of glucose triggers the generation of H_2O_2 (as is shown in the green region by the gray circle in the right image in Figure 3C) to enhance HRP's motion within the region filled with H_2O_2. The HRP that is more than 5 μm away from Gox shows no significant different motion compared with the first group. The lateral motion of HRP is enhanced as the substrate concentration increases within a close range, further illustrating the cascade reaction facilitates an enhanced diffusion of enzymes. This work provides the opportunity for exploring the interaction between proteins. In addition, Klein et al. investigated the mechanism and kinetic performance of various enzyme configurations in cascade reactions based on the TOA (Klein et al., 2019). As is shown in Figure 3D, three kinds of enzymes are anchored on one arm of TOA to conduct the cascade reaction. The turnover rates versus two factors (maltoheptaose concentration and NADH) for various combinations of tri-enzymes assembled on TOA in different ratios and positions are evaluated from the theoretical and experimental point of view. In this work, due to the enhanced stability of the enzymes, as well as DNA affinity and hydration layer effect, a nearly 30-fold enhancement of the enzyme activity of tri-enzymes loaded on TOA was observed compared with that of tri-enzymes diffusing freely in solution. This method provided the opportunity to design more complicated cascade systems and study the mechanism and kinetic performance of multiple enzyme systems.

Enzymatic cascade systems based on 3D DNA nanostructures

3D DNA nanostructures provide powerful tools to explore the catalytic performance of enzymatic cascade systems due to their 3D-confined environment. Folding the 2D DNA nanostructure into 3D tubular DNA origami promotes the study of controlling biocatalytic cascade reactions (Fu et al., 2013). Fu et al. tried to assemble GOx/HRP on ROA with staples on edges for folding the 2D DNA nanostructure into 3D tubular DNA origami. The connection between bi-enzymes is strengthened due to the low diffusion of substrates within the tubular origami, resulting in the enhanced catalytic activity of the cascade system. Another bi-enzyme system constructed on a 3D DNA origami cage was presented by Yan's group (Zhao et al., 2016). As is shown in Figure 3E, the HRP and GOx are encapsulated within two half-origami cages, respectively. Then, the extended captures at the edge of half-origami cages combine the two cages together via DNA hybridization, assisting the integration of the enzymatic cascade system. The enzymatic activity of biocatalytic cascade reaction fabricated within 3D DNA origami cage exhibits 3-fold enhancement, which is higher than that of freestanding bi-enzyme system. The enzymatic cascade systems based on 3D DNA nanostructures may open up opportunities for protecting the enzymes from the degradation by protease and also may mimic the local surroundings of enzymes in biological systems.

APPLICATIONS OF DNA-BASED ENZYMATIC SYSTEMS IN SENSING AND BIOMEDICINE
In vitro detection based on DNA-assembled enzymatic systems

Dzs-based sensors can work as a promising candidate for ion detection *in vitro*, including Mg^{2+}, Ni^+, Na^+, Zr^{2+}, K^+, and so on (Wu et al., 2017; Liu et al., 2021b; Chen et al., 2017; McConnell et al., 2021; Cheng et al., 2020, 2021; Ren et al., 2020). Liu's group developed a lanthanide-specific Dzs array for the separation of lanthanides from non-lanthanides (Huang et al., 2016). They used five kinds of Dzs that respond to the same substrate to identify the Lanthanides with high efficacy. This work offers a clear insight into the effectiveness of utilizing various Dzs to generate pattern-based identification of different samples. Zhou et al. designed a target-triggered Dz walker to detect copper in serum based on a Cu^{2+}-specific Dz (Zhou et al., 2021). The copper species in serum activated the catalysis of Cu^{2+}-specific Dzs, which cleaves FAM-tagged Cu-Dz substrate, resulting in the recovery of the fluorescence signal. Each walk of Cu^{2+}-specific Dzs accompanies the release of FAM-tagged fragments and the recovery of fluorescence, which acts as the monitoring signal for the 3D walking. This approach with highly enhanced detectability provides a promising potential for the exploration of Cu metabolism-related diseases.

Dzs can also be fabricated on paper- or plastic-based devices, which can be used as biosensors to detect bacteria and nucleic acids. Didar's group developed an *E. coli*-specific RCA probe marked by fluorophore on cyclo-olefin polymer film for monitoring pathogen in meat (Figure 4A) (Yousefi et al., 2018). The Dz-based sensor holds steady in 14 days within a wide pH range and achieves a limit of detection (LOD) as low as 10^3 CFU/mL for the *E. coli* detection in meat and apple juice. Recently, they have successfully
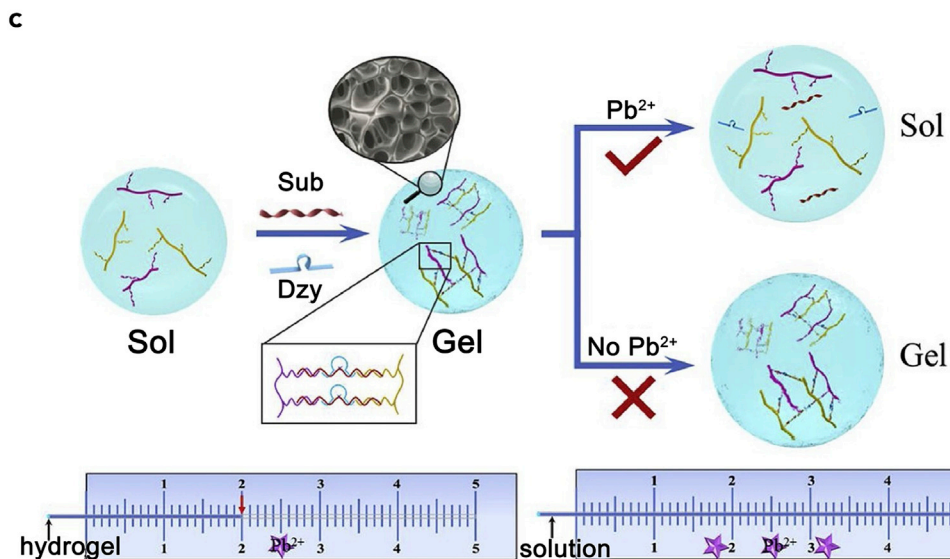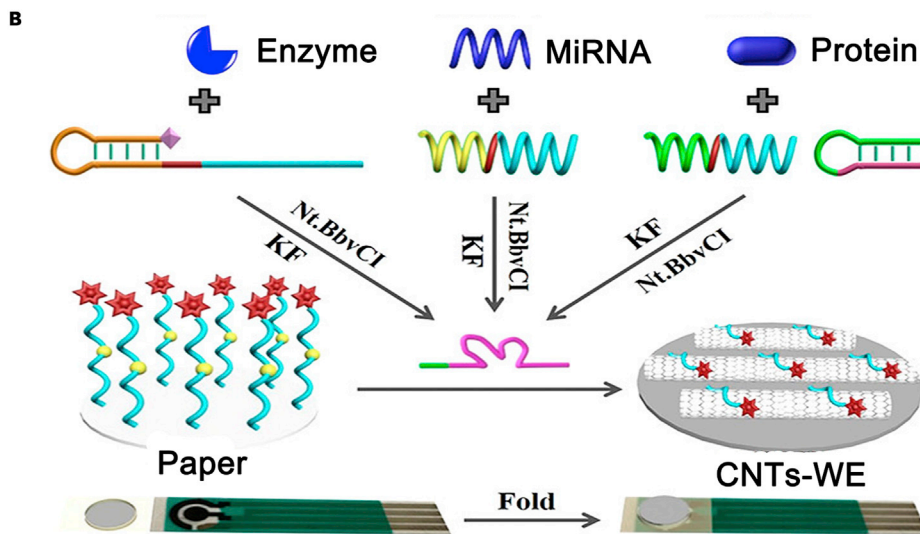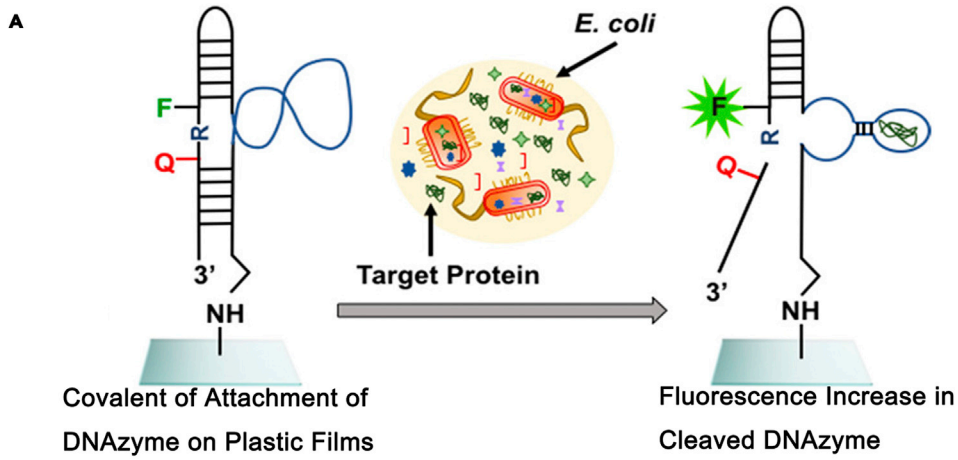
Figure 4. Representative Dz-based biosensors for pathogens and metal-ion detections

(A) Principle of sensitive Dzs-based sensors in the presence of live *E. coli* cells. Reproduced with permission (Yousefi et al., 2018). Copyright 2018, American Chemical Society.

(B) Scheme of the process of miRNA assay using the paper-based electrochemical sensor (PES) fabricated by Dzs. Reproduced with permission (Liu et al., 2019). Copyright 2019, American Chemical Society.

(C) Scheme of a portable Dz-based device for Pb^{2+} detection using a visual reading of capillary flow. Reproduced with permission (Jiang et al., 2020). Copyright 2020, Elsevier.

immobilized bacteria-responsive and fluorogenic Dzs onto lubricant-infused surfaces to construct a Dzs-based biosensor for pathogens detection within milk (Yousefi et al., 2021). The slippery surface effectively reduces the nonspecific adhesion and biofouling of the designed RCDs-based biosensor applied in complex samples, improving the cleave efficiency and sensitivity of the Dzs. The real-time monitoring of pathogens can effectively reduce the deaths and injuries caused by pathogens in food. Therefore, due to the low cost and high sensitivity of the developed pathogen-specific Dzs, the obtained Dzs-based sensor facilitates their integrations into production technology for further practical detection of pathogens in food and high payback for manufacturers. Ail et al. designed a colorimetric *Helicobacter pylori* (HP)-specific Dz-based sensor using a urease-based litmus method for the detection of HP in human stool samples (Ali et al., 2019). In the presence of bacteria, DNA-cleavage Dzs cause the urine-modified ssDNA to move to the detection region with deposited litmus, resulting in the color change. This reported Dz probe for detecting HP possesses advantages of low cost, portable ability, and detection efficiency, which is expected to be used to prevent the health issues caused by pathogen infections. Liu et al. reported an Mg^{2+}-dependent Dzs-based sensor, which can perform efficient detection for microRNA-21 (miR-21) based on the electrochemical paper (Figure 4B) (Liu et al., 2019). The target miR-21 is hybridized to the ssDNA probe, which can be extended to dsDNA by KF polymerase. The resultant dsDNA is cleaved by nicking endonuclease to release the Mg^{2+}-dependent Dz strand. The Dz strands spontaneously fold to form an active loop-included conformation and hybridize with the ferrocene-labeled DNA on paper. The Mg^{2+} triggers the releases of ferrocene-labeled DNA fragments, which can adsorb onto the carbon-nanotube-modified screen-printed electrode, resulting in the enhanced electrical signal. This Mg^{2+}-dependent Dzs-based paper sensor realizes sensitive detection of miR-21 with relatively low background.

Various approaches have been developed to construct the intelligent and portable device based on Dzs and surface-enhanced Raman spectroscopy (SERS). In 2019, Wang et al. reported a portable SERS-based sensor with the assistant of uranyl-selective Dzs for the detection of uranyl in the river and tap water (He et al., 2019). The uranyl-selective Dzs are tagged with 50-rhodamine B (RhB) as SERS reporters. Once the Dzs are cleaved by the target, the RhB-tagged fragment can be released and hybridize with its complementary DNA on 3D ZnO-Ag mesoporous nanosheet with three separate SERS biochips. Strong SERS signals were monitored due to the incremental adjacency between the RhB reporters and the surface of the SERS biochips. This Dzs-based device possesses high sensitivity and high detection speed and reach a limit of detection for uranyl at the fM level. In addition, a portable visual capillary sensor for Pb^{2+} detection based on Pb^{2+}-dependent Dzs (i.e., GR-5) was reported by Jiang et al. (2020). As is shown in Figure 4C, the cross-linking of the GR-5 Dzs induces the polyacrylamide-nucleic acids to self-assemble into a hydrogel, which is motionless in the capillary tube. With the addition of Pb^{2+}, the substrate encapsulated in the hydrogel is cleaved by GR-5 Dzs, leading to the disassembly of the hydrogel. This process undergoes a transition from hydrogel to solution, resulting in the detectable migration in the capillary tube. The addition amount of Pb^{2+} has a positive influence on the moving distance in the capillary tube with a proportional relation. This portable sensor allows the detection of Pb^{2+} in tap water with high sensitivity and specificity, which can also be further used in molecular diagnostics or analyte detection in food.

Intracellular and *in vivo* applications of DNA-based enzymatic systems

Metal-dependent Dzs can be used to regulate the interactions between cells. Lu's group demonstrated the Dzs-controlled cell dynamic system to manipulate the cell-cell motion (Qian et al., 2021). As depicted in Figure 5A, the 5′-end of Dz and its substrates are modified with cholesterol to insert into the phospholipid layer on the surface of two groups of living cells via hydrophobic interactions. The other end of Dz is labelled with a fluorophore for tracking. Two kinds of Dzs and their substrates are added and located on the surface of different living cells. Zn^{2+}-specific and Mg^{2+}-specific Dzs are simultaneously assembled between cells, inducing the cell-cell aggregation. The right images in Figure 5A displayed the changeable cell-cell behavior under the regulation of Dzs. With the addition of specific metal ions, the corresponding sequence can be cleaved, inducing the disconnection between two cell spheroids. It is demonstrated that
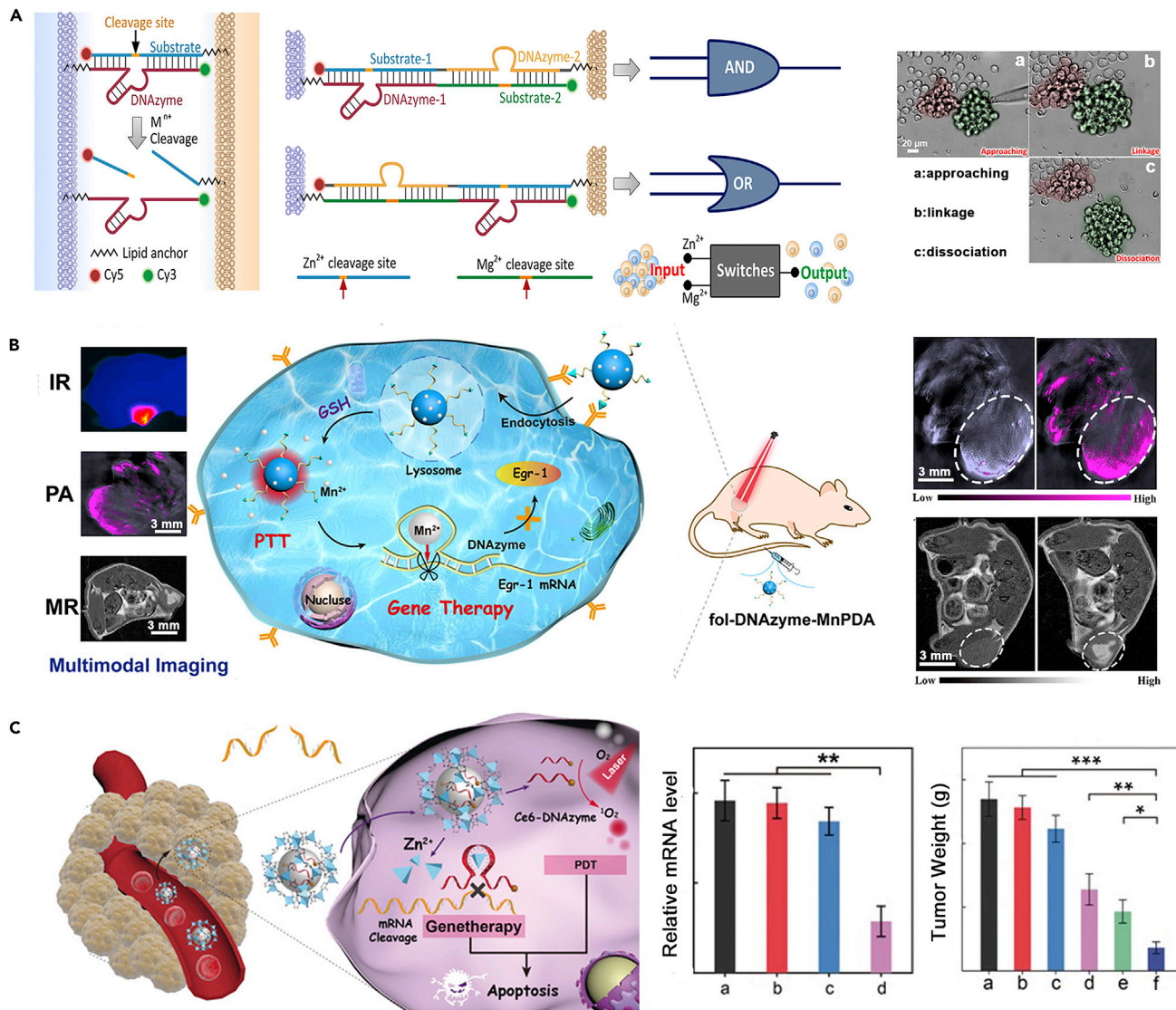
Figure 5. Dzs-based enzymatic systems for the cell motion and gene therapy

(A) Cell-cell interaction based on Dzs. Reproduced with permission (Qian et al., 2021). Copyright 2021, American Chemical Society.

(B) Scheme of fol-Dz-MnPDA nanoplatform for multimodal imaging-guided therapy. Reproduced with permission (Feng et al., 2018). Copyright 2018, American Chemical Society.

(C) Dz@ZIF-8 nanosystem for fluorescence imaging and gene/photodynamic therapy. Reproduced with permission (Wang et al., 2019). Copyright 2019, Wiley-VCH.

the addition of two kinds of metal ions for different Dzs can control the DNA double-chain switches, which provides an intelligent tool to regulate dynamic cell behaviors.

Recently, researchers have been devoted to developing the applications of DNA-based enzymatic systems in biosensing, bioimaging, and biotherapy *in vivo*. A representative work presented by Lu's group in 2018 reported a Zn^{2+}-dependent Dz for intracellular Zn^{2+} detection (Yang et al., 2018). The Dz-based probe conjugated on lanthanide-doped up-conversion nanoparticles (UCNPs) can be excited by the near-infrared (NIR) in living cells and zebrafish embryos. Furthermore, Wang's group demonstrated a biological circuit based on Mn^{2+}-specific, autocatalytic Dzs for miRNA imaging in mice (Wei et al., 2020). The circuit includes a honeycomb MnO_2 nanosponge (hMNS) and the substrate of RCD. In the presence of GSH, the hMNS can release Mn^{2+}, which acts as a cofactor for the Dz and the magnetic resonance imaging (MRI) contrast

regent. The intracellular miRNA-21 triggers the hybridization chain reaction (HCR) reactions, generating DNA nanowires containing Dzs units. The generated Dzs cleave the Mn^{2+}-selected substrates and produce new triggers for the feedback of HCR. Consequently, with the combination of cross-feedback of HCR and Dz-based cleavage, the designed system realizes an amplified signal of miRNA. This hMNS-based Dz probe can realize high sensitivity for miRNA detection by signal amplification effect and also make contributions to its further application for miRNA detection *in vivo* with high spatial resolution. Another interesting study reported by Xiong et al. realizes the detection of intracellular metal ions by a genetically encoded sensor based on metal-ion-specific RCD (Xiong et al., 2020). The plasmids including two genetically encoded fluorescent proteins (FPs) (Clover2 and Ruby2) and inactive trans-acting Dzs are transfected into the Hela cell. The Dzs with RNA-cleavage ability can inhibit the expression of Clover2 FP by cleaving the Clover2 mRNA, whereas the expression of the red fluorescent protein mutant Ruby2 FP is not affected. The relatively equal expression of Clover2 FP and Ruby2 FP is interrupted, inducing the emergence of unbalanced fluorescent signals. Specifically, they used two kinds of RNA-cleaving Dzs to modulate the expression of fluorescent proteins, including Mg^{2+}-specific 10–23 Dzs and Zn^{2+}-specific 8–17 Dzs, respectively. Based on this reported mechanism, this strategy also provides opportunities to detect other intracellular metal ions by using regioselective metal-dependent Dzs.

For further applying the DNA-based catalytic systems in biotherapy, Wang's group designed a folate-labeled Dz-polydopamine-Mn^{2+} nanoparticle, which simultaneously realized multimodal imaging and gene therapy *in vivo* (Figure 5B) (Feng et al., 2018). In the presence of intracellular GSH, the nanoparticles decompose and release Mn^{2+}, which is the cofactor of the Dzs for mRNA cleavage, resulting in gene silence and tumor growth inhibition. As is shown in Figure 5B (right), these nanoparticles induce clear photoacoustic imaging (PAI) and MRI signals *in vivo*. In addition, the desirable photothermal transduction efficiency and gene silence ability of these nanoparticles endow them to be a promising candidate for tumor therapy. Moreover, the same group reported another Zn^{2+}-based Dz encapsulated in the metal-organic framework (MOF), which is able to cleave the human early growth response-1 (EGR-1) mRNA to reduce the EGR-1 mRNA expression (Figure 5C) (Wang et al., 2019). By the integration of photodynamic therapy (PDT) with gene therapy, the tumors are inhibited to a great degree. Recently, Yang's group reported an ultra-long DNA sequence containing repeated Mn^{2+}-specific Dz sequences for enhanced gene therapy by regulating the catalytic performance of the NIR-light-driven Dzs *in vivo* (Zhao et al., 2021). Here, MnO_2 nanoparticles with polydopamine coating were assembled on the surface of DNA nanostructures that can respond to GSH and release Mn^{2+} to activate the Mn^{2+}-specific Dzs, cleaving the target EGR-1 mRNA. Meanwhile, the desirable photothermal conversion ability of polydopamine can promote the temperature increase of tumor sites to enhance the activity of Dzs, further facilitating gene therapy. This work achieves the regulation of the activity of Dzs *in vivo* by the light-conversion method for an effective gene therapy that exhibits great potential in clinical applications. Subsequently, Yang's group designed a DNA nanoscaffold for synergistic gene therapy by combining Mn^{2+}-selected Dzs and CRISPR/Cas9 system (Li et al., 2022). They designed an ultra-long ssDNA containing the sequences of Cas9/sgRNA recognition regime, the selected Dzs, and HhaI restriction sites. This ultra-long ssDNA can be compressed by Mn^{2+} to form DNA nanoscaffold. The surface of the obtained DNA nanostructure is modified with HhaI coated with acid degradable polymers. The exposed and acid-responsive HhaI enzyme triggers the release of Cas9/sgRNA and Dzs in the acidic lysosome. With the help of cofactor Mn^{2+} and the favorable delivery efficiency caused by DNA scaffolds, Dzs with RNA-cleavage ability assist the CRISPR/Cas9 to achieve the synergistic and high-efficient gene therapy. In addition, a Dz-controlled enzymatic system (Dz13) demonstrated by Meng et al. was used for gene regulation to inhibit the growth of squamous cell carcinomas (Meng et al., 2019). This system is designed based on the tetrahedral DNA nanostructures (TDNs) as the delivery platform. TDN modified with a 5' end-extended Dz13 sequence performs a high intracellular uptake efficiency of Dz13. With the desired accumulation of Dz13 in cells, highly active Dz13 triggers the cleavage of c-Jun mRNA, which is related to cell proliferation, transformation, and apoptosis, to suppress the growth of cancer cells via gene silencing. The combination of high-biocompatible DNA nanostructures as carriers and Dzs for effective gene therapy provides inspiration for utilizing the DNA-based enzymatic platforms as nucleic acid drugs to promote the gene therapy.

CHALLENGES AND PERSPECTIVES

Taking advantage of extraordinary programmability, both DNA molecules and DNA nanostructures can be utilized for the construction of DNA-based enzymatic systems. The DNA-based enzymatic systems can be applied in different fields, such as environmental monitoring and disease theranostics. Although the DNA-

based enzymatic systems exhibit great potential in many application fields, there still remain several challenges:

(1) The stability of Dzs under the complicated biological environment is one of the important issues. Dzs tend to be degraded by nuclease, and the functions of Dzs may be interfered by proteins that exist in the physiological environment. In order to prolong the circulation time of Dzs and maintain the activity of Dzs in the complex physiological matrix, the integration of Dzs with DNA nanostructures may be a possible approach to protect the Dzs from being cleaved by endonucleases. In 2019, Wu's group presented a tetrahedron-based Dzs biosensor for intracellular miRNA detection (Li et al., 2019). The DNA tetrahedron with high biocompatibility and flexibility were used as the carrier to deliver the Dzs into cells with high nuclease resistance and excellent cell permeability. Due to their desirable cell penetration ability and structural stability, more and more Dzs-based biosensors using DNA nanostructures as carriers have been fabricated, which open up new horizons for the efficient delivery of Dzs at the cellular level and provide new opportunities for further tumor therapy (Meng et al., 2019; Ren et al., 2019). Moreover, the modification of Dzs with unnatural nucleotides is another promising strategy to enhance Dzs' stability, which has already been utilized in the development of nucleic acid drugs (Wang et al., 2021b; Damha et al., 1998). For instance, Wang et al. have accomplished a novel xeno-nucleic-acid-modified 10–23 Dz for enhanced resistance of nuclease digestion and persistent activity in the physiological environment (Wang et al., 2021b). The new type 10–23 Dz contains three kinds of nucleic acid, including DNA, 2'-fluoroarabino nucleic acids (FANA) and α-L-threofuranosyl nucleic acid (TNA), wherein the fluorine atom at the 2' position of a 2'-deoxyarabinose sugar in FANA is designed to alleviate the nuclease digestion. In addition, TNA possesses a modified four-carbon threose sugar, which can maintain the stability of the backbone structure. Therefore, the xeno-nucleic-acid-modified 10–23 Dz is endowed with fantastic stability and enhanced activity in the complex physiological environment, which can promote its application for future clinical use.

(2) More Dzs should be screened for the detection of various substrates *in vitro* and *in vivo* with enhanced activity. Compared with the divalent metal ion-dependent Dzs (M^{2+}) that have been widely reported, few Dzs with high specificity for monovalent metal ions (M^+), especially *in vivo*, have been investigated (Torabi et al., 2015). A possible reason is that most M^+ ions lack ample affinity and specificity of binding with Dzs (Sarkar et al., 2014; Dubach et al., 2011). For instance, the low selectivity and sensitivity of Na^+-specific Dzs can be interfered by other M^+ ions (e.g., K^+) to restrict the intracellular Na^+ detection efficiency (Geyer and Sen, 1997). To overcome this obstacle, efforts are required for the development of novel catalytic core sequence of the Dzs, which possess higher sensitivity for target ions and molecules. One feasible strategy is the combination of Dzs with sequence-specific aptamers, which can achieve higher affinity for substrates, thereby increasing the catalytic activity of Dzs (Saran et al., 2017).

(3) The catalytic mechanisms of different Dzs should be further clarified in order to obtain higher catalytic performances by tuning the sequence design parameters rationally. Recently, Victor et al. used 10–23 Dz as the model to study high-resolution structural characteristics of the relevant status of the Dzs during the catalytic process (Borggräfe et al., 2022). The molecular conformation of Dzs has been firstly characterized with high temporal resolution at the atomic level. The monitoring of the dynamic changes of the Dzs happening in the catalytic process helps understand the Dzs activity deeper and clearer, which provides a more detailed theoretical basis to design various Dzs with optimized properties to realize their potential applications.

In summary, Dzs bear a plethora of advantages, such as easy fabrication, low cost, and high tolerance to thermal and pH change compared with traditional protein-based enzymes. Therefore, the Dzs are excellent candidates that can work in harsh environments where are not compatible to the conventional biocatalysts, thus allowing Dz-based catalytic systems to be used for wide biological applications. DNA molecules and DNA nanostructures provide versatile platforms to fabricate enzymatic systems that can generate various functions in complex environments. The integration of functional Dzs and DNA nanostructures to fabricate the DNA-based enzymatic platforms endows the regulated activity, cellular delivery, and addressable positioning ability for complicated *in vivo* applications. Through the selection of DNA sequences and rational design of the DNA nanostructures, these enzymatic systems will play more important roles in environmental detection, chemical sensing, and disease treatments. With more and more efforts paid in this field,

the fast development of DNA-based catalytic devices would promote the emergence of versatile applications.

AUTHOR CONTRIBUTIONS

Yunfei Jiao and Yingxu Shang wrote this review. Na Li and Baoquan Ding supervised this review. All authors made contributions to discuss, revise, and proof this review.

DECLARATION OF INTERESTS

The authors declare no competing financial interest.

REFERENCES

Ali, M.M., Wolfe, M., Tram, K., Gu, J., Filipe, C.D.M., Li, Y., and Brennan, J.D. (2019). A DNAzyme-based colorimetric paper sensor for *Helicobacter pylori*. Angew. Chem. Int. Ed. *58*, 9907–9911.

Aranda, J., Terrazas, M., Gómez, H., Villegas, N., and Orozco, M. (2019). An artificial DNAzyme RNA ligase shows a reaction mechanism resembling that of cellular polymerases. Nat. Catal. *2*, 544–552.

Atsumi, H., and Belcher, A.M. (2018). DNA origami and G-quadruplex hybrid complexes induce size control of single-walled carbon nanotubes via biological activation. ACS Nano *12*, 7986–7995.

Borggräfe, J., Victor, J., Rosenbach, H., Viegas, A., Gertzen, C.G.W., Wuebben, C., Kovacs, H., Gopalswamy, M., Riesner, D., Steger, G., et al. (2022). Time-resolved structural analysis of an RNA-cleaving DNA catalyst. Nature *601*, 144–149.

Breaker, R.R., and Joyce, G.F. (1994). A DNA enzyme that cleaves RNA. Chem. Biol. *1*, 223–229.

Brown, A.K., Li, J., Pavot, C.M.B., and Lu, Y. (2003). A lead-dependent DNAzyme with a two-step mechanism. Biochemistry *42*, 7152–7161.

Camden, A.J., Walsh, S.M., Suk, S.H., and Silverman, S.K. (2016). DNA oligonucleotide 3′-phosphorylation by a DNA enzyme. Biochemistry *55*, 2671–2676.

Chandra, M., Sachdeva, A., and Silverman, S.K. (2009). DNA-catalyzed sequence-specific hydrolysis of DNA. Nat. Chem. Biol. *5*, 718–720.

Chen, J., Guo, Y., Zhou, J., and Ju, H. (2017). The effect of adenine repeats on G-quadruplex/hemin peroxidase mimicking DNAzyme activity. Chem. Eur. J. *23*, 4210–4215.

Chen, J., Zhang, Y., Cheng, M., Guo, Y., Sponer, J., Monchaud, D., Mergny, J.-L., Ju, H., and Zhou, J. (2018a). How proximal nucleobases regulate the catalytic activity of G-quadruplex/hemin DNAzymes. ACS Catal. *8*, 11352–11361.

Chen, Y., Ke, G., Ma, Y., Zhu, Z., Liu, M., Liu, Y., Yan, H., and Yang, C.J. (2018b). A synthetic light-driven substrate channeling system for precise regulation of enzyme cascade activity based on DNA origami. J. Am. Chem. Soc. *140*, 8990–8996.

Cheng, Y., Cheng, M., Hao, J., Jia, G., Monchaud, D., and Li, C. (2020). The noncovalent dimerization of a G-quadruplex/hemin DNAzyme improves its biocatalytic properties. Chem. Sci. *11*, 8846–8853.

Cheng, Y., Cheng, M., Hao, J., Miao, W., Zhou, W., Jia, G., and Li, C. (2021). Highly selective detection of K+ based on a dimerized G-quadruplex DNAzyme. Anal. Chem. *93*, 6907–6912.

Cuenoud, B., and Szostak, J.W. (1995). A DNA metalloenzyme with DNA ligase activity. Nature *375*, 611–614.

Damha, M.J., Wilds, C.J., Noronha, A., Brukner, I., Borkow, G., Arion, D., and Parniak, M.A. (1998). Hybrids of RNA and Arabinonucleic acids (ANA and 2′F-ANA) are substrates of ribonuclease H. J. Am. Chem. Soc. *120*, 12976–12977.

Du, P., Xu, S., Xu, Z.K., and Wang, Z.G. (2021). Bioinspired self-assembling materials for modulating enzyme functions. Adv. Funct. Mater. *31*, 2104819.

Du, P.-D., Liu, S.Y., Sun, H., Wu, H.F., and Wang, Z.-G. (2022). Designed histidine-rich peptide self-assembly for accelerating oxidase-catalyzed reactions. Nano Res. https://doi.org/10.1007/s12274-022-4209-6.

Dubach, J.M., Lim, E., Zhang, N., Francis, K.P., and Clark, H. (2011). *In vivo* sodium concentration continuously monitored with fluorescent sensors. Integr. Biol. *3*, 142–148.

Feng, J., Xu, Z., Liu, F., Zhao, Y., Yu, W., Pan, M., Wang, F., and Liu, X. (2018). Versatile catalytic deoxyribozyme vehicles for multimodal imaging-guided efficient gene regulation and photothermal therapy. ACS Nano *12*, 12888–12901.

Fu, J., Liu, M., Liu, Y., Woodbury, N.W., and Yan, H. (2012). Interenzyme substrate diffusion for an enzyme cascade organized on spatially addressable DNA nanostructures. J. Am. Chem. Soc. *134*, 5516–5519.

Fu, J., Yang, Y.R., Johnson-Buck, A., Liu, M., Liu, Y., Walter, N.G., Woodbury, N.W., and Yan, H. (2014). Multi-enzyme complexes on DNA scaffolds capable of substrate channelling with an artificial swinging arm. Nat. Nanotechnol. *9*, 531–536.

Fu, T.J., and Seeman, N.C. (1993). DNA double-crossover molecules. Biochemistry *32*, 3211–3220.

Fu, Y., Zeng, D., Chao, J., Jin, Y., Zhang, Z., Liu, H., Li, D., Ma, H., Huang, Q., Gothelf, K.V., and Fan, C. (2013). Single-step rapid assembly of DNA origami nanostructures for addressable nanoscale bioreactors. J. Am. Chem. Soc. *135*, 696–702.

Geyer, C.R., and Sen, D. (1997). Evidence for the metal-cofactor independence of an RNA phosphodiester-cleaving DNA enzyme. Chem. Biol. *4*, 579–593.

Guo, Y., Chen, J., Cheng, M., Monchaud, D., Zhou, J., and Ju, H. (2017). A thermophilic tetramolecular G-quadruplex/hemin DNAzyme. Angew. Chem. Int. Ed. *56*, 16636–16640.

He, X., Wang, S., Liu, Y., and Wang, X. (2019). Ultra-sensitive detection of uranyl ions with a specially designed high-efficiency SERS-based microfluidic device. Sci. China Chem. *62*, 1064–1071.

Hoang, M., Huang, P.-J., and Liu, J. (2015). G-quadruplex DNA for fluorescent and colorimetric detection of Thallium(I). ACS Sensors *1*, 137–143.

Hollenstein, M. (2015). DNA catalysis: the chemical repertoire of DNAzymes. Molecules *20*, 20777–20804.

Huang, P.-J., Vazin, M., Lin, J., Pautler, R., and Liu, J. (2016). Distinction of individual lanthanide ions with a DNAzyme beacon array. ACS Sensors *1*, 732–738.

Huang, P.-J.J., De Rochambeau, D., Sleiman, H.F., and Liu, J. (2020). Target self-enhanced selectivity in metal-specific DNAzymes. Angew. Chem. Int. Ed. *59*, 3573–3577.

Jiang, C., Li, Y., Wang, H., Chen, D., and Wen, Y. (2020). A portable visual capillary sensor based on functional DNA crosslinked hydrogel for point-of-care detection of lead ion. Sens. Actuators B Chem. *307*, 127625–127633.

Khachigian, L.M. (2019). Deoxyribozymes as catalytic nanotherapeutic agents. Cancer Res. *79*, 879–888.

Klein, W.P., Thomsen, R.P., Turner, K.B., Walper, S.A., Vranish, J., Kjems, J., Ancona, M.G., and Medintz, I.L. (2019). Enhanced catalysis from multienzyme cascades assembled on a DNA origami triangle. ACS Nano *13*, 13677–13689.

Kumar, S., Jain, S., Dilbaghi, N., Ahluwalia, A.S., Hassan, A.A., and Kim, K.-H. (2019). Advanced selection methodologies for DNAzymes in sensing and healthcare applications. Trends Biochem. Sci. *44*, 190–213.

Kurapati, R., and Bianco, A. (2018). Peroxidase mimicking DNAzymes degrade graphene oxide. Nanoscale *10*, 19316–19321.

Li, C., Xue, C., Wang, J., Luo, M., Shen, Z., and Wu, Z.-S. (2019). Oriented tetrahedron-mediated protection of catalytic DNA molecular-scale detector against in vivo degradation for intracellular miRNA detection. Anal. Chem. *91*, 11529–11536.

Li, F., Song, N., Dong, Y., Li, S., Li, L., Liu, Y., Li, Z., and Yang, D. (2022). A proton-activatable DNA-based nanosystem enables co-delivery of CRISPR/Cas9 and DNAzyme for combined gene therapy. Angew. Chem. Int. Ed. *61*, e202116569.

Li, W., Li, Y., Liu, Z., Lin, B., Yi, H., Xu, F., Nie, Z., and Yao, S. (2016). Insight into G-quadruplex-hemin DNAzyme/RNAzyme: adjacent adenine as the intramolecular species for remarkable enhancement of enzymatic activity. Nucleic Acids Res. *44*, 7373–7384.

Li, Y., and Breaker, R.R. (1999). Phosphorylating DNA with DNA. Proc. Nat. Acad. Sci. U S A *96*, 2746–2751.

Lin, Y., Yang, Z., Lake, R.J., Zheng, C., and Lu, Y. (2019). Enzyme-mediated endogenous and bioorthogonal control of a DNAzyme fluorescent sensor for imaging metal ions in living cells. Angew. Chem. Int. Ed. *58*, 17061–17067.

Linko, V., Eerikäinen, M., and Kostiainen, M.A. (2015). A modular DNA origami-based enzyme cascade nanoreactor. Chem. Commun. *51*, 5351–5354.

Liu, C., Chen, Y., Zhao, J., Wang, Y., Shao, Y., Gu, Z., Li, L., and Zhao, Y. (2021a). Self-assembly of copper–DNAzyme nanohybrids for dual-catalytic tumor therapy. Angew. Chem. Int. Ed. *60*, 14324–14328.

Liu, C., Chen, Y., Zhao, J., Wang, Y., Shao, Y., Gu, Z., Li, L., and Zhao, Y. (2021b). Self-assembly of copper–DNAzyme nanohybrids for dual-catalytic tumor therapy. Angew. Chem. *133*, 14445–14449.

Liu, K., Lat, P.K., Yu, H.-Z., and Sen, D. (2020a). CLICK-17, a DNA enzyme that harnesses ultra-low concentrations of either Cu+ or Cu2+ to catalyze the azide-alkyne 'click' reaction in water. Nucleic Acids Res. *48*, 7356–7370.

Liu, M., Zhang, Q., Chang, D., Gu, J., Brennan, J.D., and Li, Y. (2017a). A DNAzyme feedback amplification strategy for biosensing. Angew. Chem. Int. Ed. *56*, 6142–6146.

Liu, Q., Wang, H., Shi, X., Wang, Z.-G., and Ding, B. (2017b). Self-assembled DNA/Peptide-Based nanoparticle exhibiting synergistic enzymatic activity. ACS Nano *11*, 7251–7258.

Liu, S., Du, P., Sun, H., Yu, H.-Y., and Wang, Z.-G. (2020b). Bioinspired supramolecular catalysts from designed self-assembly of DNA or peptides. ACS Catal. *10*, 14937–14958.

Liu, W., Zhong, H., Wang, R., and Seeman, N.C. (2011). Crystalline two-dimensional DNA-origami arrays. Angew. Chem. Int. Ed. *50*, 264–267.

Liu, X., Li, X., Gao, X., Ge, L., Sun, X., and Li, F. (2019). A universal paper-based electrochemical sensor for zero-background assay of diverse biomarkers. ACS Appl. Mater. Inter. *11*, 15381–15388.

McConnell, E.M., Cozma, I., Mou, Q., Brennan, J.D., Lu, Y., and Li, Y. (2021). Biosensing with DNAzymes. Chem. Soc. Rev. *50*, 8954–8994.

Meng, L., Ma, W., Lin, S., Shi, S., Li, Y., and Lin, Y. (2019). Tetrahedral DNA nanostructure-delivered DNAzyme for gene silencing to suppress cell growth. ACS Appl. Mater. Inter. *11*, 6850–6857.

Mergny, J.-L., and Sen, D. (2019). DNA quadruple helices in nanotechnology. Chem. Rev. *119*, 6290–6325.

Morrison, D., Rothenbroker, M., and Li, Y. (2018). DNAzymes: selected for applications. Small Methods *2*, 1700319.

Ngo, T.A., Nakata, E., Saimura, M., and Morii, T. (2016). Spatially organized enzymes drive cofactor-coupled cascade reactions. J. Am. Chem. Soc. *138*, 3012–3021.

Peng, H., Li, X.-F., Zhang, H., and Le, X.C. (2017). A microRNA-initiated DNAzyme motor operating in living cells. Nat. Commun. *8*, 14378–14391.

Ponce-Salvatierra, A., Wawrzyniak-Turek, K., Steuerwald, U., Höbartner, C., and Pena, V. (2016). Crystal structure of a DNA catalyst. Nature *529*, 231–234.

Poon, L.C.H., Methot, S.P., Morabi-Pazooki, W., Pio, F., Bennet, A.J., and Sen, D. (2011). Guanine-rich RNAs and DNAs that bind heme robustly catalyze oxygen transfer reactions. J. Am. Chem. Soc. *133*, 1877–1884.

Praetorius, F., Kick, B., Behler, K.L., Honemann, M.N., Weuster-Botz, D., and Dietz, H. (2017). Biotechnological mass production of DNA origami. Nature *552*, 84–87.

Purtha, W.E., Coppins, R.L., Smalley, M.K., and Silverman, S.K. (2005). General deoxyribozyme-catalyzed synthesis of native 3′−5′ RNA linkages. J. Am. Chem. Soc. *127*, 13124–13125.

Qian, R.-C., Zhou, Z.-R., Guo, W., Wu, Y., Yang, Z., and Lu, Y. (2021). Cell surface engineering using DNAzymes: metal ion mediated control of cell–cell interactions. J. Am. Chem. Soc. *143*, 5737–5744.

Ren, T., Deng, Z., Liu, H., Li, X., Li, J., Yuan, J., He, Y., Liu, Q., Yang, Y., and Zhong, S. (2019). Co-delivery of DNAzyme and a chemotherapy drug using a DNA tetrahedron for enhanced anticancer therapy through synergistic effects. New J. Chem. *43*, 14020–14027.

Ren, W., Jimmy Huang, P.-J., De Rochambeau, D., Moon, W.J., Zhang, J., Lyu, M., Wang, S., Sleiman, H., and Liu, J. (2020). Selection of a metal ligand modified DNAzyme for detecting Ni2+. Biosens. Bioelectron. *165*, 112285–112292.

Rothemund, P.W.K. (2006). Folding DNA to create nanoscale shapes and patterns. Nature *440*, 297–302.

Santoro, S.W., and Joyce, G.F. (1997). A general purpose RNA-cleaving DNA enzyme. Proc. Nat. Acad. Sci. U S A *94*, 4262–4266.

Saran, R., Kleinke, K., Zhou, W., Yu, T., and Liu, J. (2017). A silver-specific DNAzyme with a new silver aptamer and salt-promoted activity. Biochemistry *56*, 1955–1962.

Sarkar, A.R., Heo, C.H., Park, M.Y., Lee, H.W., and Kim, H.M. (2014). A small molecule two-photon fluorescent probe for intracellular sodium ions. Chem. Commun. *50*, 1309–1312.

Schlosser, K., Gu, J., Sule, L., and Li, Y. (2008). Sequence-function relationships provide new insight into the cleavage site selectivity of the 8–17 RNA-cleaving deoxyribozyme. Nucleic Acids Res. *36*, 1472–1481.

Seeman, N.C. (1982). Nucleic acid junctions and lattices. J. Theor. Biol. *99*, 237–247.

Silverman, S.K. (2016). Catalytic DNA: scope, applications, and biochemistry of deoxyribozymes. Trends Biochem. Sci. *41*, 595–609.

Sun, L., Gao, Y., Xu, Y., Chao, J., Liu, H., Wang, L., Li, D., and Fan, C. (2017). Real-time imaging of single-molecule enzyme cascade using a DNA origami raft. J. Am. Chem. Soc. *139*, 17525–17532.

Sun, Y., Shi, L., Wang, Q., Mi, L., and Li, T. (2019). Spherical nucleic acid enzyme (SNAzyme) boosted chemiluminescence miRNA imaging using a smartphone. Anal. Chem. *91*, 3652–3658.

Tikhomirov, G., Petersen, P., and Qian, L. (2017). Fractal assembly of micrometre-scale DNA origami arrays with arbitrary patterns. Nature *552*, 67–71.

Torabi, S.-F., Wu, P., Mcghee, C.E., Chen, L., Hwang, K., Zheng, N., Cheng, J., and Lu, Y. (2015). In vitro selection of a sodium-specific DNAzyme and its application in intracellular sensing. Proc. Nat. Acad. Sci. U S A *112*, 5903–5908.

Travascio, P., Li, Y., and Sen, D. (1998). DNA-enhanced peroxidase activity of a DNA aptamer-hemin complex. Chem. Biol. *5*, 505–517.

Vázquez-González, M., WANG, C., and WILLNER, I. (2020). Biocatalytic cascades operating on macromolecular scaffolds and in confined environments. Nat. Catal. *3*, 256–273.

Virgilio, A., Esposito, V., Lejault, P., Monchaud, D., and Galeone, A. (2020). Improved performances of catalytic G-quadruplexes (G4-DNAzymes) via the chemical modifications of the DNA backbone to provide G-quadruplexes with double 3'-external G-quartets. Int. J. Biol. Macromol. *151*, 976–983.

Wang, H., Chen, Y., Wang, H., Liu, X., Zhou, X., and Wang, F. (2019). DNAzyme-loaded metal–organic frameworks (MOFs) for self-sufficient gene therapy. Angew. Chem. Int. Ed. *58*, 7380–7384.

Wang, J., Cheng, M., Chen, J., Ju, H., Monchaud, D., Mergny, J.-L., and Zhou, J. (2020). An oxidatively damaged G-quadruplex/hemin DNAzyme. Chem. Commun. *56*, 1839–1842.

Wang, Q., Tan, K., Wang, H., Shang, J., Wan, Y., Liu, X., Weng, X., and Wang, F. (2021a). Orthogonal demethylase-activated deoxyribozyme for intracellular imaging and gene regulation. J. Am. Chem. Soc. *143*, 6895–6904.

Wang, Y., Nguyen, K., Spitale, R.C., and Chaput, J.C. (2021b). A biologically stable DNAzyme that efficiently silences gene expression in cells. Nat. Chem. *13*, 319–326.

Wang, Z.-G., Liu, Q., and Ding, B. (2014). Shape-controlled nanofabrication of conducting polymer on planar DNA templates. Chem. Mater. *26*, 3364–3367.

Wang, Z.-G., Wilner, O.I., and Willner, I. (2009). Self-assembly of aptamer–circular DNA nanostructures for controlled Biocatalysis. Nano Lett. *9*, 4098–4102.

Wei, B., Dai, M., and Yin, P. (2012). Complex shapes self-assembled from single-stranded DNA tiles. Nature *485*, 623–626.

Wei, J., Wang, H., Wu, Q., Gong, X., Ma, K., Liu, X., and Wang, F. (2020). A smart, autocatalytic, DNAzyme biocircuit for in vivo, amplified, microRNA imaging. Angew. Chem. Int. Ed. *59*, 5965–5971.

Winterwerber, P., Harvey, S., Ng, D.Y.W., and Weil, T. (2020). Photocontrolled dopamine polymerization on DNA origami with nanometer resolution. Angew. Chem. Int. Ed. *59*, 6144–6149.

Wu, Z., Fan, H., Satyavolu, N.S.R., Wang, W., Lake, R., Jiang, J.-H., and Lu, Y. (2017). Imaging endogenous metal ions in living cells using a DNAzyme–catalytic hairpin assembly probe. Angew. Chem. Int. Ed. *56*, 8721–8725.

Xiao, L., Gu, C., and Xiang, Y. (2019). Orthogonal activation of RNA-cleaving DNAzymes in live cells by reactive oxygen species. Angew. Chem. Int. Ed. *58*, 14167–14172.

Xin, L., Zhou, C., Yang, Z., and Liu, D. (2013). Regulation of an enzyme cascade reaction by a DNA machine. Small *9*, 3088–3091.

Xiong, M., Yang, Z., Lake, R.J., Li, J., Hong, S., Fan, H., Zhang, X.B., and Lu, Y. (2020). DNAzyme-mediated genetically encoded sensors for ratiometric imaging of metal ions in living cells. Angew. Chem. Int. Ed. *59*, 1891–1896.

Xu, J., Jiang, R., He, H., Ma, C., and Tang, Z. (2021). Recent advances on G-quadruplex for biosensing, bioimaging and cancer therapy. Trends Anal. Chem. *139*, 116257–116278.

Yang, Y., Zhang, S., Yao, S., Pan, R., Hidaka, K., Emura, T., Fan, C., Sugiyama, H., Xu, Y., Endo, M., and Qian, X. (2019). Programming rotary motions with a hexagonal DNA nanomachine. Chem. Eur. J. *25*, 5158–5162.

Yang, Z., Loh, K.Y., Chu, Y.-T., Feng, R., Satyavolu, N.S.R., Xiong, M., Nakamata Huynh, S.M., Hwang, K., Li, L., Xing, H., et al. (2018). Optical control of metal ion probes in cells and zebrafish using highly selective DNAzymes conjugated to upconversion nanoparticles. J. Am. Chem. Soc. *140*, 17656–17665.

Yousefi, H., Ali, M.M., Su, H.-M., Filipe, C.D.M., and Didar, T.F. (2018). Sentinel wraps: real-time monitoring of food contamination by printing DNAzyme probes on food packaging. ACS Nano *12*, 3287–3294.

Yousefi, H., Samani, S.E., Khan, S., Prasad, A., Shakeri, A., Li, Y., Filipe, C.D.M., and Didar, T.F. (2021). LISzyme biosensors: DNAzymes embedded in an anti-biofouling platform for hands-free real-time detection of bacterial contamination in milk. ACS Nano *16*, 29–37.

Zhang, Y., Xu, J., Zhou, S., Zhu, L., Lv, X., Zhang, J., Zhang, L., Zhu, P., and Yu, J. (2020). DNAzyme-triggered visual and ratiometric electrochemiluminescence dual-readout assay for Pb(II) based on an assembled paper device. Anal. Chem. *92*, 3874–3881.

Zhao, H., Zhang, Z., Zuo, D., Li, L., Li, F., and Yang, D. (2021). A synergistic DNA-polydopamine-MnO2 nanocomplex for near-infrared-light-powered DNAzyme-mediated gene therapy. Nano Lett. *21*, 5377–5385.

Zhao, Z., Fu, J., Dhakal, S., Johnson-Buck, A., Liu, M., Zhang, T., Woodbury, N.W., Liu, Y., Walter, N.G., and Yan, H. (2016). Nanocaged enzymes with enhanced catalytic activity and increased stability against protease digestion. Nat. Commun. *7*, 10619–10628.

Zhong, R., Xiao, M., Zhu, C., Shen, X., Tang, Q., Zhang, W., Wang, L., Song, S., Qu, X., Pei, H., et al. (2018). Logic catalytic interconversion of G-molecular hydrogel. ACS Appl. Mater. Inter. *10*, 4512–4518.

Zhou, L., Xiong, Y., Wang, H., Yin, A., Zhang, X., Li, H., Fu, Q., and Huang, P. (2021). Target-triggered DNAzyme walker with 3D walking unit for copper species sensing in serum: a multivalent binding strategy for improving the detection performance. Sens. Actuators B Chem. *334*, 129589–129597.

Zhou, W., Chen, Q., Huang, P.-J.J., Ding, J., and Liu, J. (2015). DNAzyme hybridization, cleavage, degradation, and sensing in undiluted human blood serum. Anal. Chem. *87*, 4001–4007.

Zhou, W., Saran, R., Chen, Q., Ding, J., and Liu, J. (2016). A new Na+-dependent RNA-cleaving DNAzyme with over 1000-fold rate acceleration by ethanol. Chembiochem *17*, 159–163.